Chapter 6

Results and Discussions

6.1 Luminance Detection Model Results

The theoretical details of the luminance detection models and experimental procedures have been discussed in previous chapters. Four experimental results on the K value of Kuno model, the K value of modified model, small inclination test and light metering experiment will be discussed in this section.

6.1.1 Results of Kuno Model Test

According to Kuno model, the experiments are performed to find K value. Parts of the result are plotted in **Figs. 6-1** and **6-2**, respectively. As shown in **Fig. 6-1**, K values are varied largely from 140 to 200, but the corresponding slope of mean integrated luminance signal value $\sum_m$ is steady relatively. The similar results can also be seen in **Fig. 6-2**. According to the unstable phenomenon of K value, we suppose that there should be a modified constant offset value to be appended into Kuno model. Therefore, we propose a *modified* luminance detection model by adding an offset value and another exposure parameter A (F-number). The results of the modified model are listed in next section.

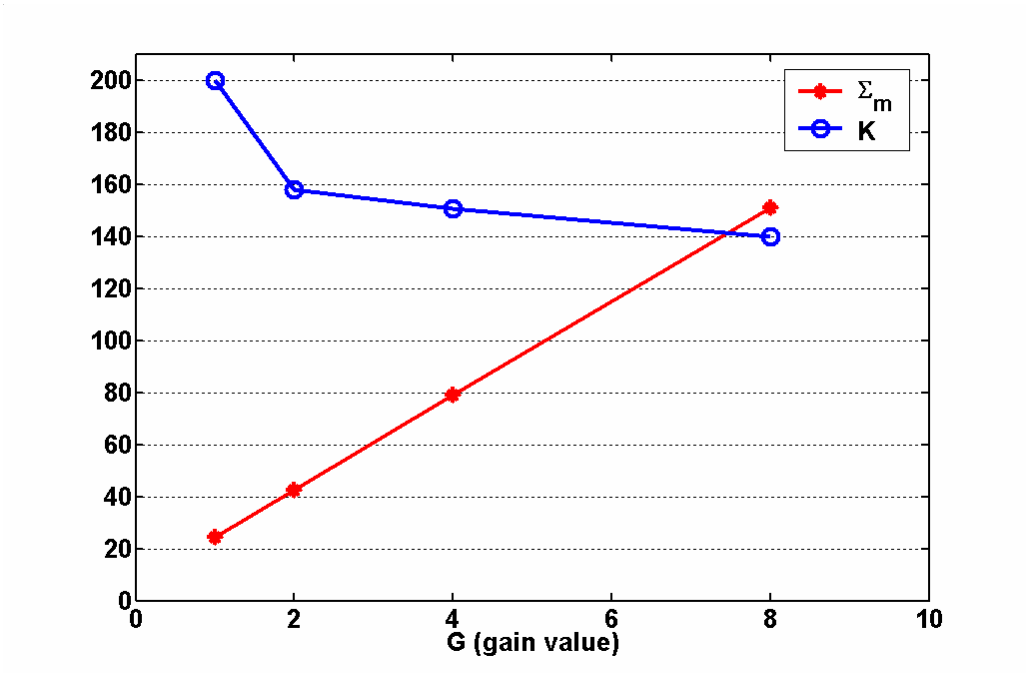

Fig. 6-1 K value of Kuno model is a function of AGC gain (G), and mean integrated luminance signal value $\sum_m$ is a function of AGC gain (G).

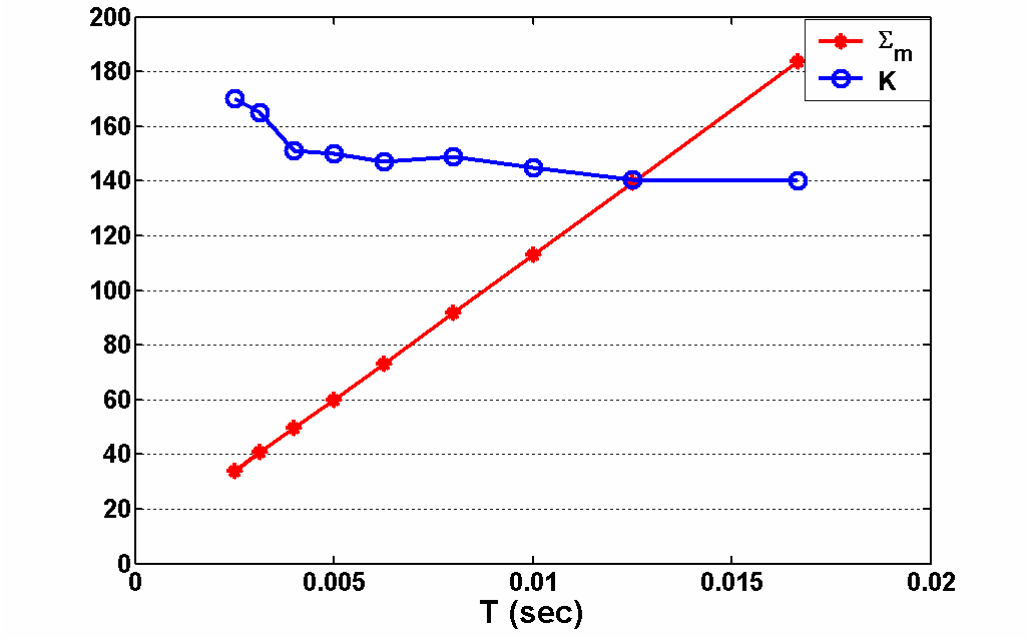

Fig. 6-2 K value of Kuno model is a function of exposure time (T), and mean integrated luminance signal value $\sum_m$ is a function of exposure time (T).

6.1.2 Results of Modified Model Test

In the examination of modified model, the experiments are performed for investigating the relation of K and offset values for different gain value (G), exposure time (T), and F-number (A). The final results are plotted in **Figs. 6-3**, **6-4** and **6-5**, individually. The variations of K and offset values are much more stable compared with the Kuno model. According to the modified model, the stability of luminance detection can be improved.

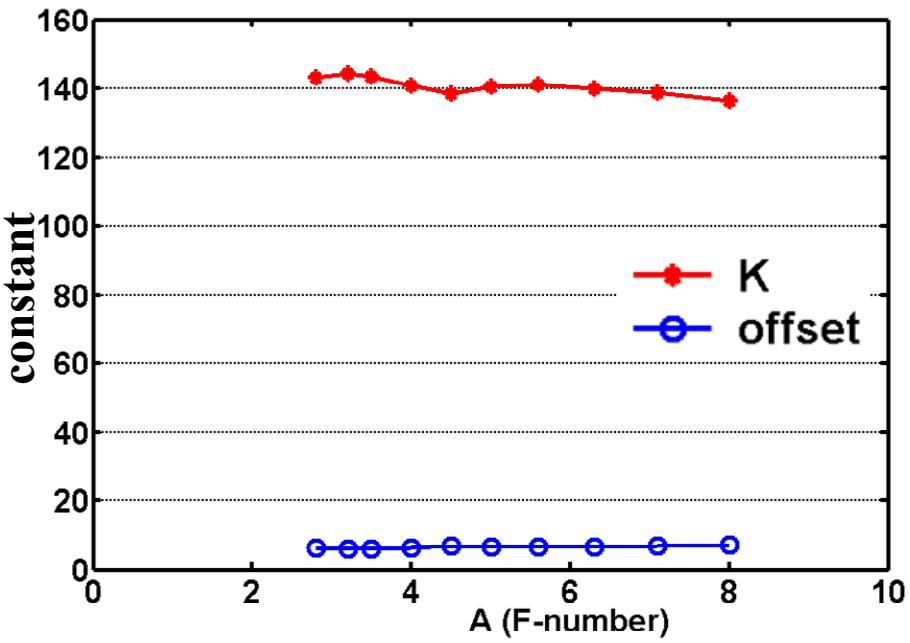

Fig. 6-3 Constant K（offset）value as a function of F-number (A)

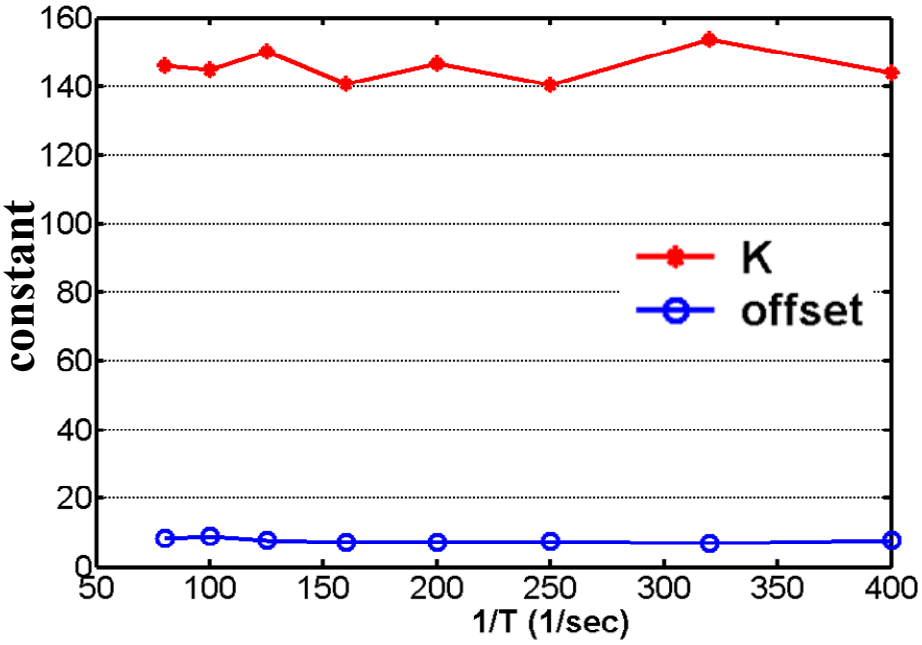

Fig. 6-4 Constant K（offset）value as a function of exposure time T

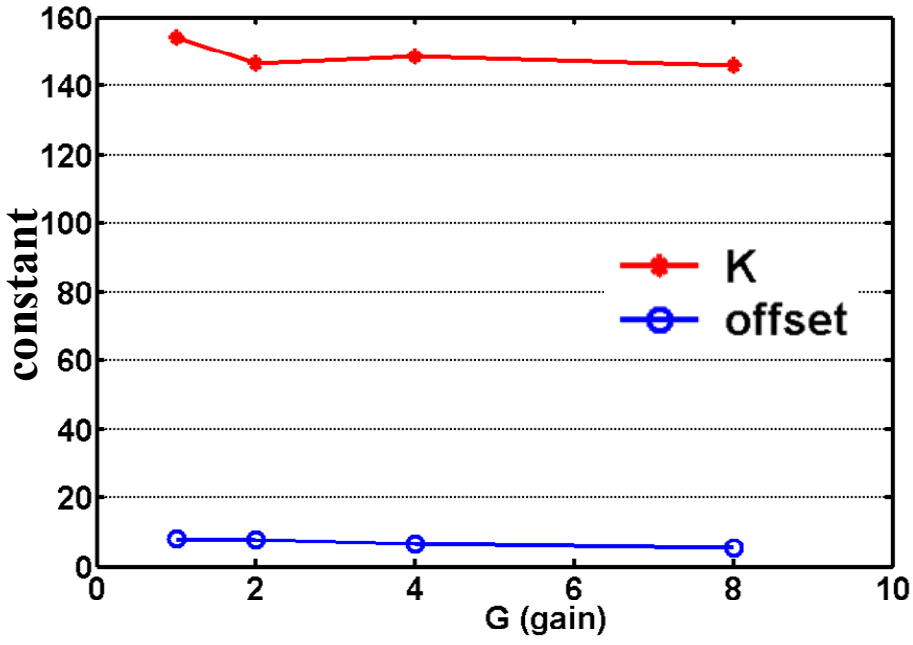

Fig. 6-5 Constant K（offset）value as a function of gain value (G)

6.1.3 Results of Small Angle Inclination Test

To test the stability of the modified light metering model, the measurement of K value with a small angle inclination of the optical axis is performed. The experiment results are plotted in **Figs. 6-6** and **6-7**, respectively. The variation of K and offset in the modified model are still stable regardless of small angle inclination of optical axis, which means that K value can be effectively deduced by our modified model.

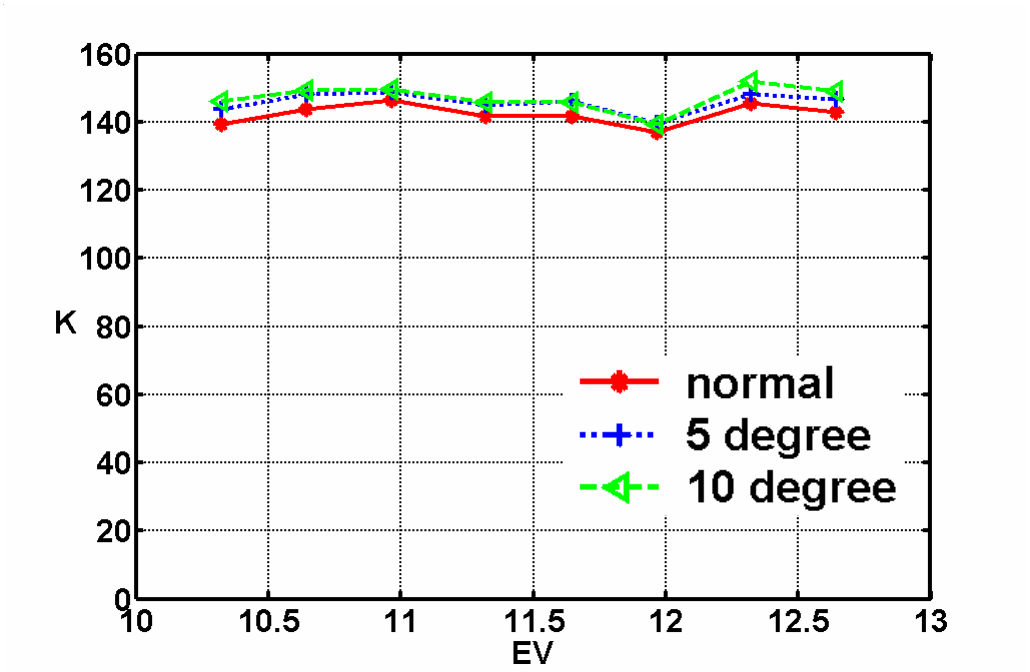

Fig. 6-6 K value as a function of EV in small angle inclination (EV = $\log_2(A^2/T)$), K value is a constant

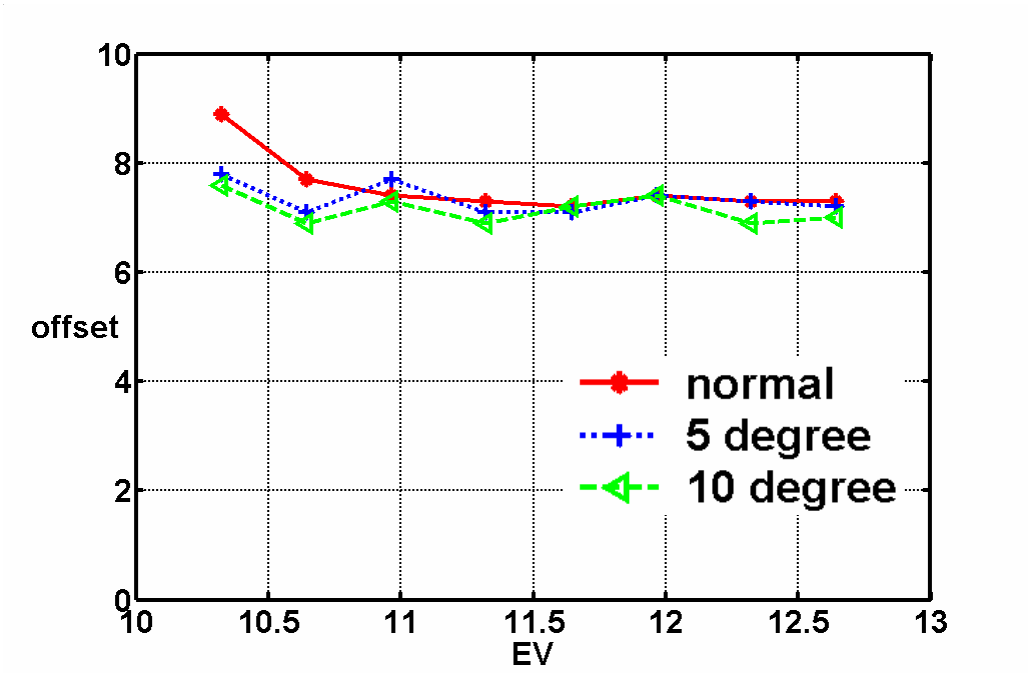

Fig. 6-7 offset value as a function of EV in small angle inclination (EV=$\log_2(A^2/T)$), offset value is a constant

6.1.4 Results of Light Metering Test

The experiments of light metering accuracy in the modified model are performed. We made experiments for different conditions under the environments from dark to bright because the dynamic range of general photographic scene varies from 10 cd/m^2 (inside a dark room) to 10^5 cd/m^2 (under the blue sky), approximately. From the measurement results listed in **Table 6-1** and shown in **Fig. 6-8**, the mean deviation between the values measured by Canon G5 and Minolta CS100 is of less than 6 %. Therefore, this modified model can easily and precisely identify the scene luminance under different environments.

Table 6-1 Light metering results of CS100 and Canon G5

Brightness conditions	Minolta CS100 (cd/m²)	Canon G5 (cd/m²)	Deviation (%)
bright ↓ dark	18400	18856	2.48%
	9000	9500	5.56%
	4530	4635	2.32%
	2270	2304	1.49%
	1140	1121	1.68%
	562	541	3.73%
	285	292	2.65%
	143	147	2.88%
	72	76	5.28%
	36	38	6.17%
	18	17	5.93%
	10	8.9	11.17%
	4.3	3.6	15.29%
Average			5.13%

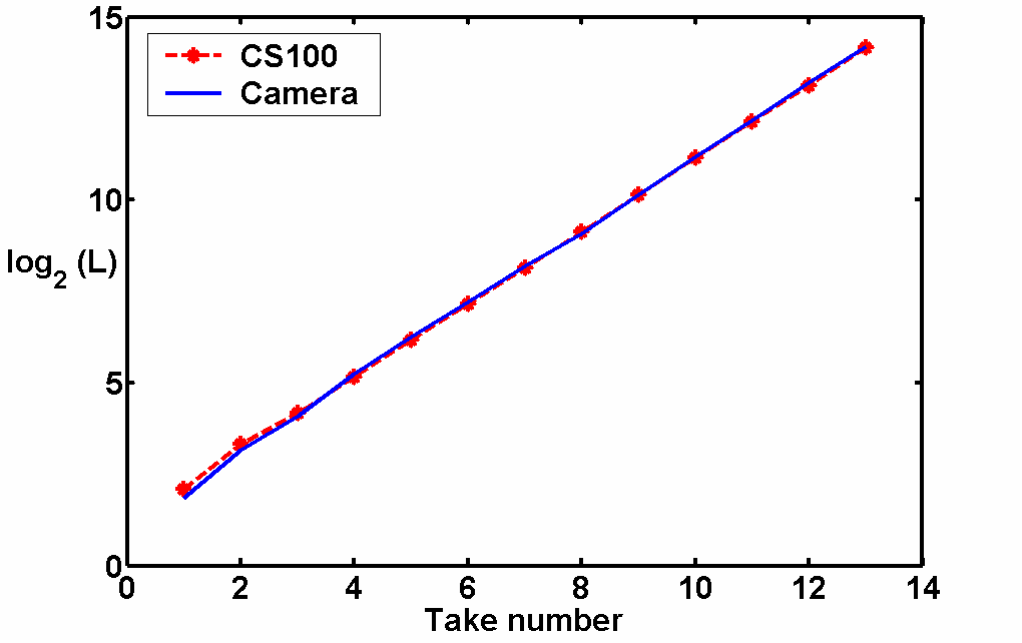

Fig. 6-8 Light metering results of CS100 and Canon G5 (L (cd/m²))

6.2 2-D Scene Analysis Method Results

The theoretical details of the proposed scene analysis method and experimental procedures have been discussed in previous chapters. Three experimental results on the optimization of database, fuzzy rules base and performance test will be discussed in this section.

6.2.1 Results of Optimization Database

According to the two optimal criterions of bound values defined in **Chapter 5**, six kinds of threshold values are determined. Besides, the optimized threshold parameters are chosen according to the results of partition as shown in **Fig. 6-9**. P% is the total percentage of the database which locates in the classified partition regions. The higher the P% value means that this kind of threshold parameters with better performance. According to the partition results, the threshold parameters of (61,194) and (46,192) have better performance. Finally, we choose (61,194) as the test parameters.

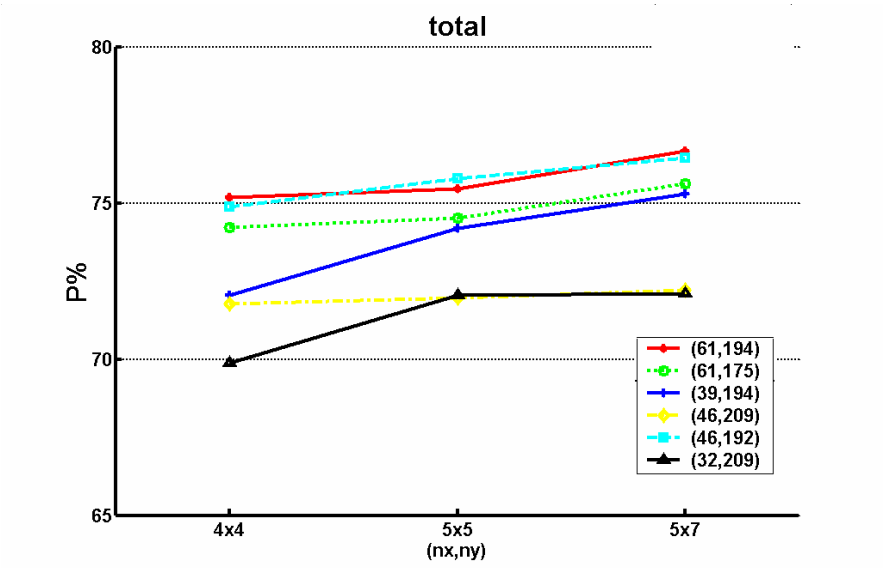

Fig. 6-9 Performance of the threshold parameters in different partition methods, nx = number of partition regions in angle axis, ny = number of partition regions in distance axis

6.2.2 Results of Fuzzy Rules Base

According to the optimized database and test parameters (61,194), we define the membership functions for each fuzzy variable. The membership functions which are determined according to the optimized database are shown in **Figs. 6-10** and **6-11**, respectively. The compensation amounts of all rules which are obtained by trial and error are listed in **Fig. 6-12**. Then, according to the membership functions and compensation amount of each rule, the defuzzified compensation amount of all regions can be evaluated by **Eqs. (4-9)** and **(4-10)**. The defuzzified compensation amounts are plotted in **Figs. 6-13** and **6-14**, respectively.

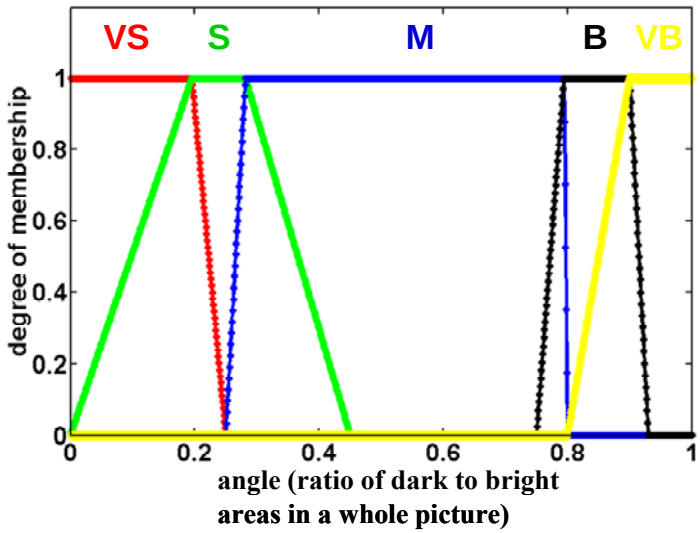

Fig. 6-10 Results of degree of membership as a function of angle and five membership functions: VS, S, M, B, VB.

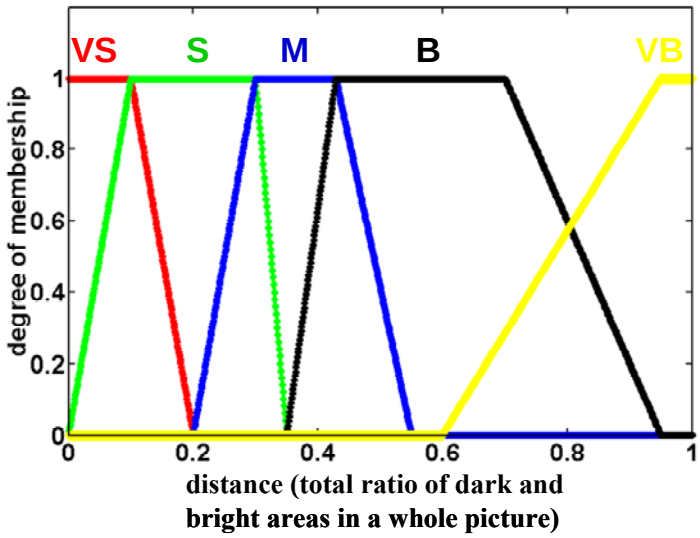

Fig. 6-11 Results of degree of membership as a function of distance and five membership functions: VS, S, M, B, VB

0	0	2	-1	1.3
0	0.3	0.7	-1	1
0	0	0	0.3	0.3
0	0	0	0	0
0	0	0	0	0

VS S M B VB

angle (ratio of dark to bright areas in a whole picture)

VS S M B VB

distance (total ratio of dark and bright areas in a whole picture)

Fig. 6-12 Results of compensation amount δEV for each region; $\delta EV = \log_2 (T_2/T_1)$, T_1: exposure time before compensation, T_2: exposure time after compensation.

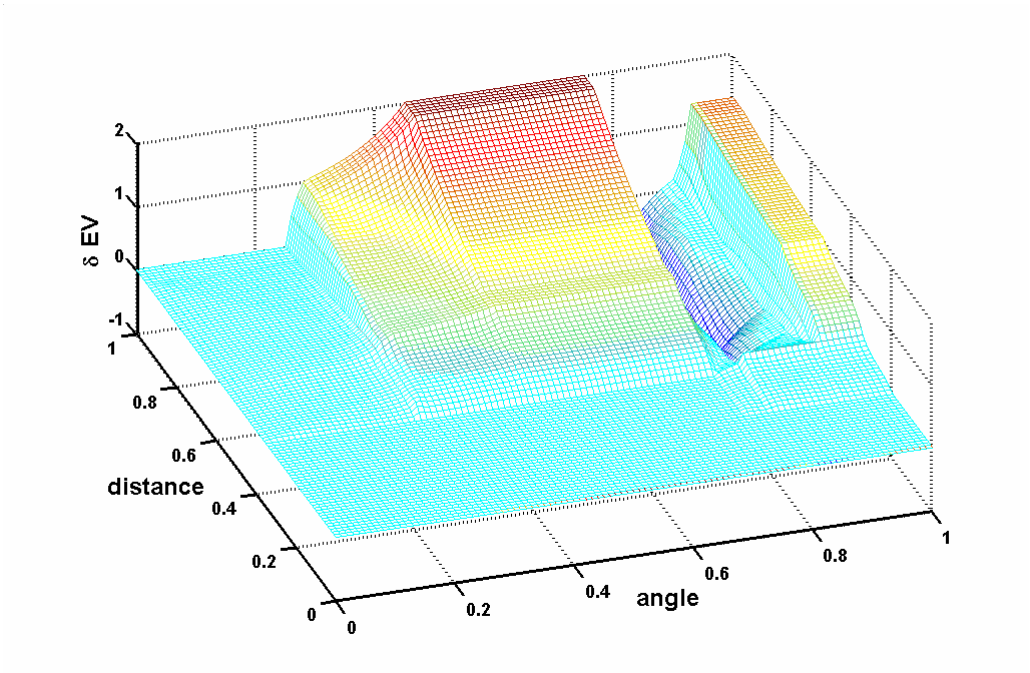

Fig. 6-13 Results of defuzzified compensation amount δEV; δEV = $\log_2 (T_2/T_1)$, T_1: exposure time before compensation, T_2: exposure time after compensation, (angle is the ratio of dark to bright areas in a whole picture, and distance is the total ratio of dark and bright areas in a whole picture.)

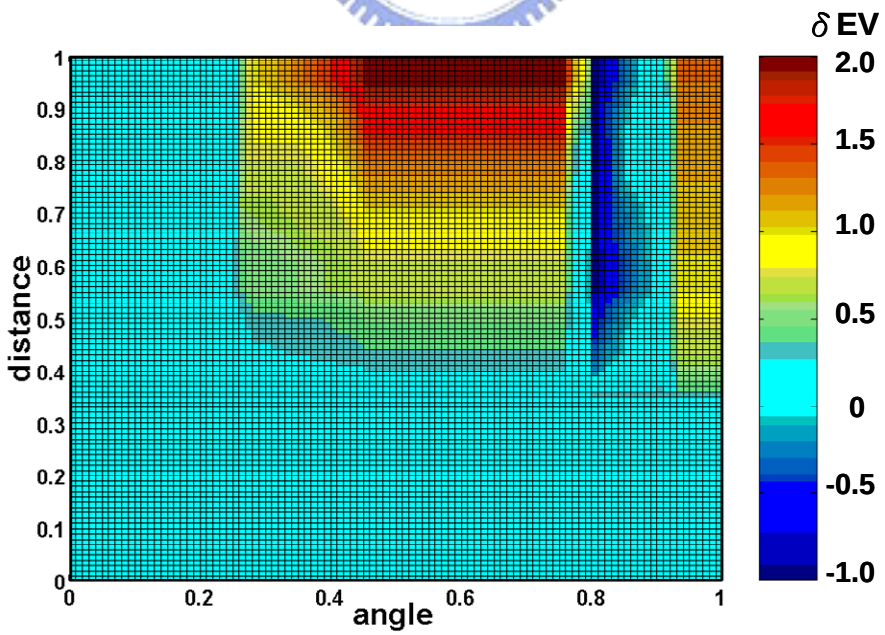

Fig. 6-14 Results of defuzzified compensation amount δEV; δEV = $\log_2 (T_2/T_1)$, T_1: exposure time before compensation, T_2: exposure time after compensation.

6.2.3 Results of Performance Test

According to the optimized database and fuzzy rules base, we examine the scene analysis method under different lighting conditions and compared with other intelligent metering methods. The comparison results are plotted in **Figs. 6-15**, **6-16**, **6-17**, **6-18**, **6-19** and **6-20**. According to the results, different lighting conditions can be detected by our scene analysis method. In the strong backlighting and backlighting conditions as shown in **Fig. 6-15** and **6-16**, we can see that the main objects of all metering modes are compensated to an acceptable level other than center-weighted metering mode. In the strong frontlighting conditions, our method does not cause error compensation as shown in **Fig. 6-17**. However, Evaluative metering mode and center-weighted metering mode + HIST analysis method cause the main object to be overexposed. In the normal conditions as shown in **Fig. 6-18**, all metering methods have proper image brightness. In the highlight situation as shown in **Fig. 6-19**, HIST analysis method causes the building to be overexposed. In the dark environment as shown in **Fig. 6-20**, our method has better exposure compensation amount. To compensate the exposure by increasing exposure time is not enough for the subject in dark environment because a flash compensation will have better image brightness.

According to the comparison results under different lighting conditions, we have confirmed that our 2-D scene analysis method can detect the images in special lighting conditions and give appropriate compensation amount. The images in backlighting, strong frontlighting and dark environment situations can be analyzed and be given with proper exposure compensation. The images in normal and highlight situations can be retained with proper brightness. Besides, the proposed method is especially suitable for the images under backlighting conditions.

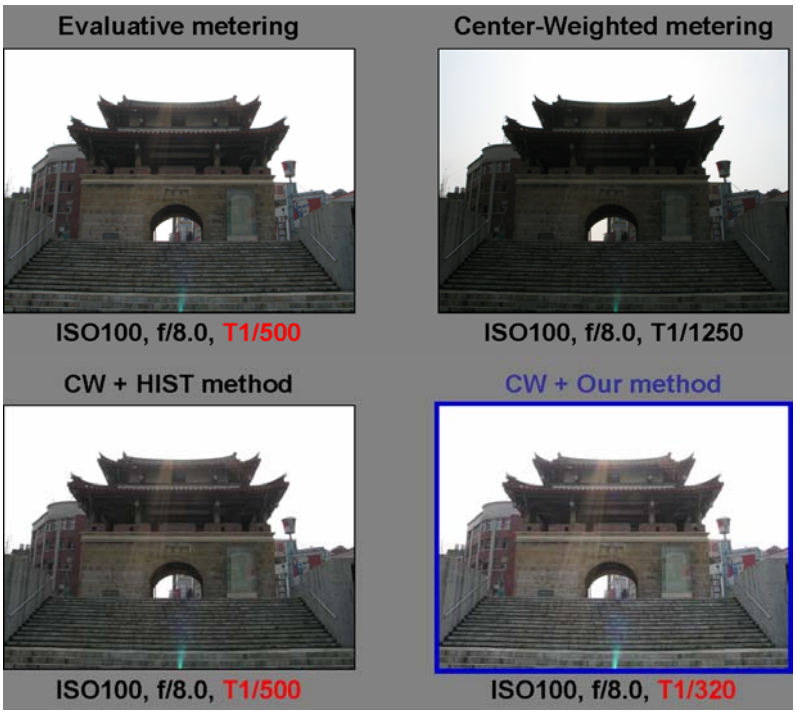

Fig. 6-15 Comparison of strong backlighting condition for different light metering methods, CW = Center-Weighted metering mode

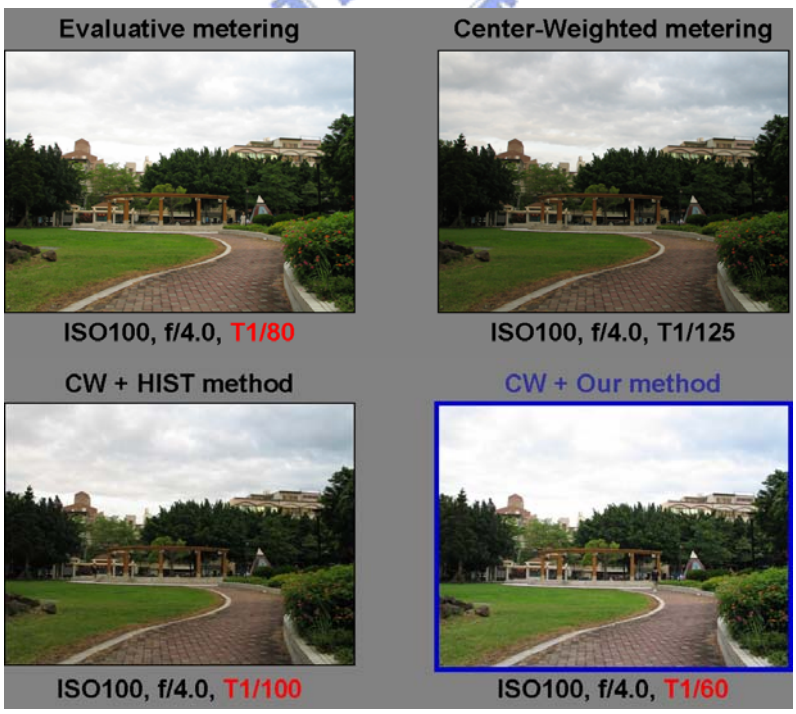

Fig. 6-16 Comparison of backlighting condition for different light metering methods

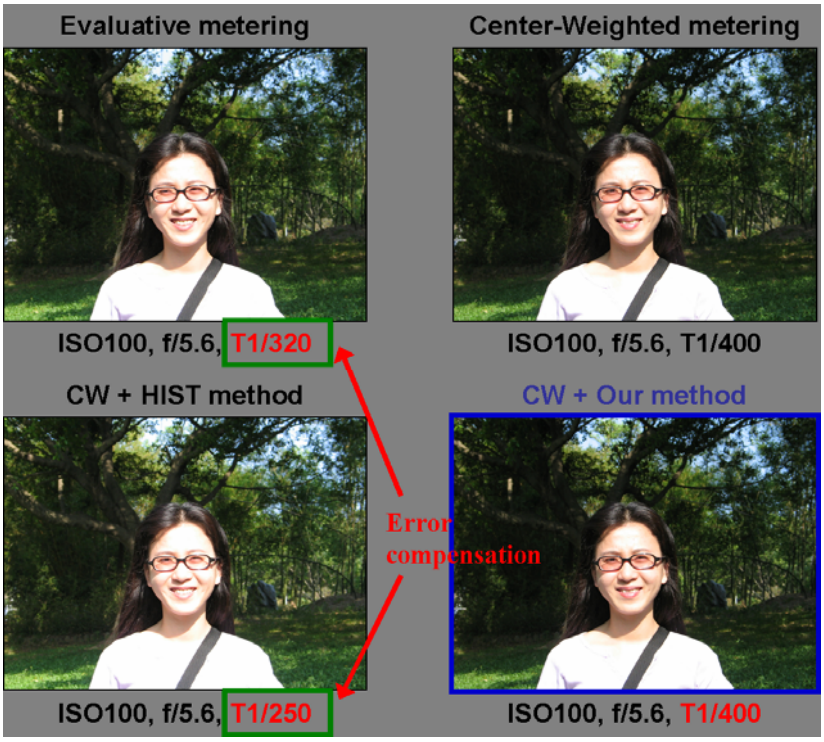

Fig. 6-17 Comparison of strong frontlighting condition for different light metering methods

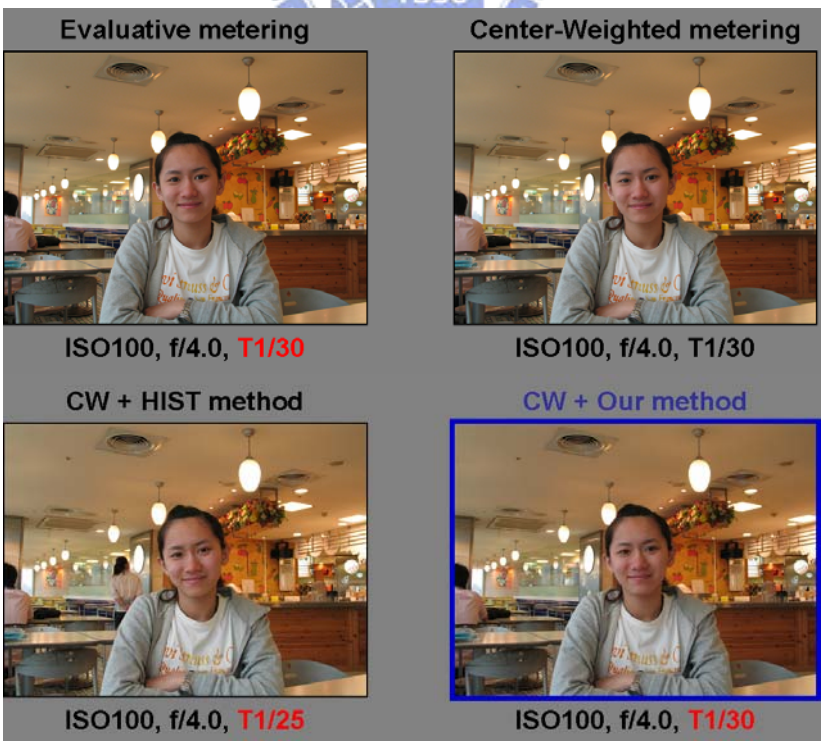

Fig. 6-18 Comparison of normal lighting condition for different light metering methods

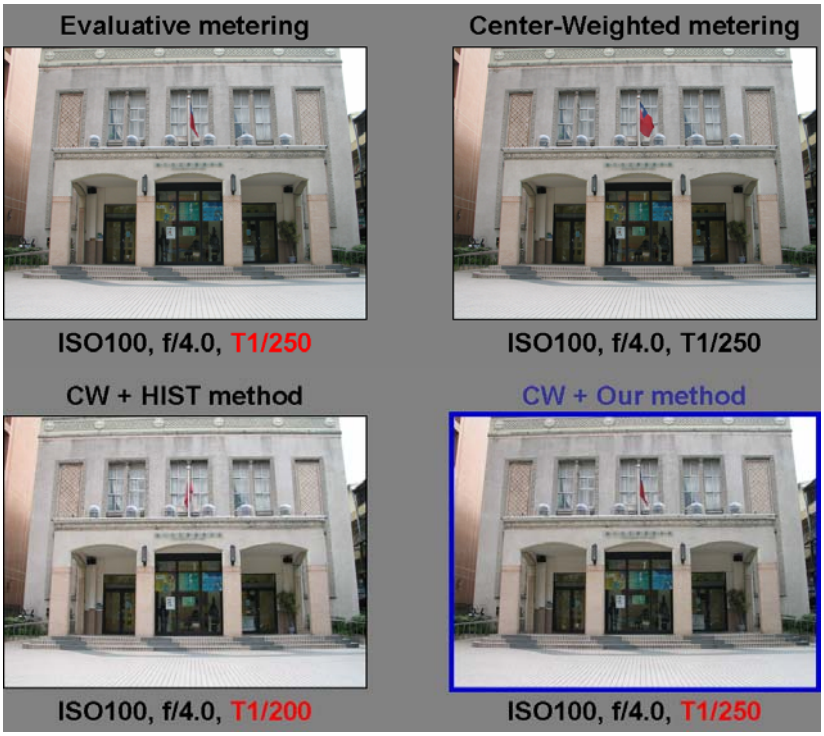

Fig. 6-19 Comparison of highlight condition for different light metering methods

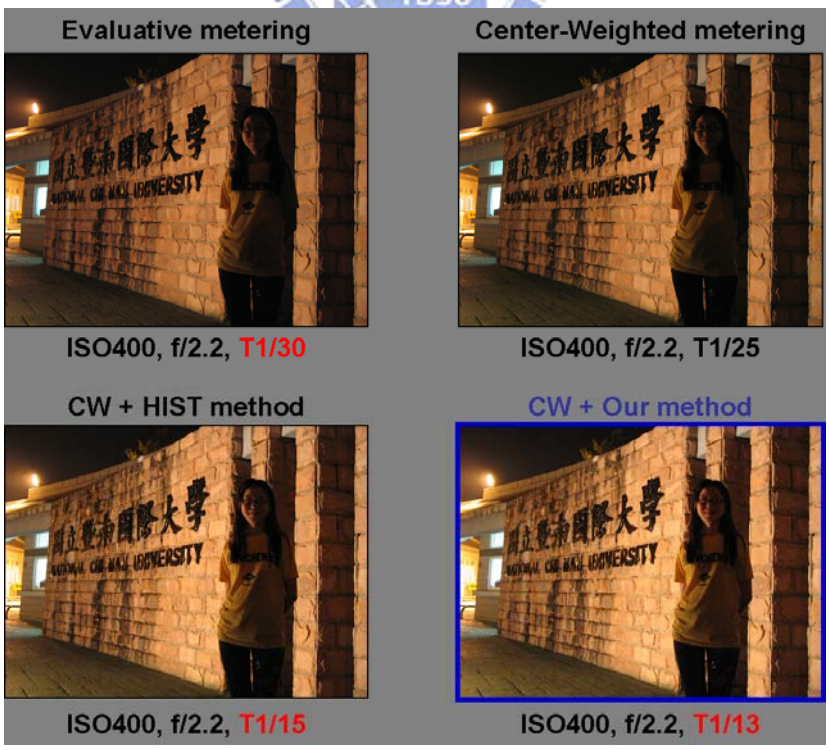

Fig. 6-20 Comparison of dark environment condition for different light metering methods

6.3 Summary

According to the proposed AE algorithms, we have done the experiments of luminance detection models and scene analysis method. From the results of proposed detection model, we have improved the stability of luminance detection model. In the comparison of different light metering methods, we have verified that our 2-D analysis method can improve the light metering ability in special lighting conditions. Therefore, the accuracy of AE system can be much improved by proposed methods.